Cathodoluminescence insights into the ionic disorder of photocatalytic anatase films

Cathodoluminescence insights into the ionic disorder of photocatalytic anatase films

Giuseppe Pezzotti[1*], Andrea Leto[2], Simone Battiston[3], Marco Minella[4], Wenliang Zhu[1]

[1]*Ceramic Physics Laboratory & Research Institute for Nanoscience, Kyoto Institute of Technology Sakyo-ku, Matsugasaki, 606-8585 Kyoto, Japan*

[2]*Piezotech Japan, Ltd., Sakyo-ku, Ichijoji, Mukaibata-cho 4, 606-8126 Kyoto, Japan*

[3]*CNR Istituto per l'Energetica e le Interfasi, Corso Stati Uniti 4, 35127 Padova, Italy*

[4]*Department of Analytical Chemistry and NIS Centre of Excellence, University of Torino, Via Giuria 5, 10125 Torino, Italy.*

[*]*Corresponding author; e-mail: pezzotti@kit.ac.jp.*

The nature of ionic disorder and the effect of structural defects on the photocatalytic function of anatase are revisited in the light of direct experimental evidence retrieved on the molecular scale by cathodoluminescence (CL) spectroscopy. CL spectra, collected on different types of photocatalytically efficient or inefficient anatase films, embodied a composite optical response of electron-compensating majority types of ionic disorder in the anatase lattice. This paper describes the dual experimental output obtained by systematically monitoring optically active off-stoichiometry sites, as follows: (i) quantitative analyses of film stoichiometry including the interactions of different lattice-defect populations; and, (ii) stability/evolution of off-stoichiometry sites upon post-fabrication annealing cycles and their effects on the photocatalytic activity of the films. CL experiments provided us with direct access to the structural state of the defective anatase lattice, thus unfolding some missing detail about the complex physicochemical interactions behind its photocatalytic efficiency.

I. INTRODUCTION

Oxygen off-stoichiometry covers a pivotal role in the complex cascade of events related to the dissociation of organic molecules by TiO_2 films.[1] Being the result of the overall ionic defect (or electronic carrier) concentration, oxygen off-stoichiometry is thus one of the most crucial properties to be controlled (or adjusted) for the optimization/improvement of the photo-electrochemical functions of the oxide.[2] The presence in TiO_2 films of both oxygen vacancies and Ti^{3+} sites has been indeed experimentally proved and their individual kinetics/energetics elucidated.[1-3], but their optimum concentrations are yet under debate and the details of their interaction conspicuously missing. Moreover, there are clear hints that the photocatalytic efficiency of TiO_2 films strongly depends on the obtainment of an appropriate defect-chemical balance.[4-6] Liu et al.[4] suggested that oxygen vacancies and Ti^{3+} sites could commonly act as hole traps which, combining with photogenerated holes, inhibit recombination of electron-hole pairs. Consequently, the defective sites become the charged species with the function of providing trapped holes for photocatalytic activity, while successively recovering to their original defective state. However, in reviewing the recent literature that describes the photocatalytic response of TiO_2, one might come across a complex and sometime controversial prospect, including a number of apparently contradictory results. Oxygen vacancies themselves introduced into pure anatase films during deposition or after it (i.e., by post-deposition annealing in hydrogen atmosphere) were systematically reported to induce red-shifted photoresponse, but they had only in some cases a positive influence on photo-reactivity.[4,7,8] Dissolution of aliovalent cations with valencies both lower (*p*-type doping; e.g., Al^{3+}, Cr^{3+}, Ga^{3+}, Ln^{3+}) and higher (*n*-type doping; e.g., Nb^{5+}, Ta^{5+}, Sb^{5+}) than that of Ti^{4+} in the TiO_2 lattice has been systematically pursued in the attempt of increasing the concentration of trapping sites

(for an exhaustive review paper see Ref.[9]). Dopants effectively alter the defect-chemical balance and generally expand the light-absorption capability of the TiO_2 photocatalyst. However, in some cases, they also increase the recombination rate of hole/electron pairs and thus degrade its photocatalytic efficiency. Studies of photocatalytic efficiency in N^{3-}-anion-doped titania films (in comparison with pristine samples) revealed that improved photocatalytic efficiencies arise not only from the formation of localized states below the conduction band edge (i.e., through the formation of color centers associated with oxygen vacancies[1]), but also from the concurrent circumstance that dopant sites should act as stabilizing entities for hole/electron pairs.[10] As a matter of fact, monovalent sodium ions (Na^+) (e.g., diffusing from glass substrates), despite being efficient promoters of oxygen vacancy formation, are labeled as "poisoning" agents for photocatalytic anatase films,[11] their detrimental effect being attributed to the quick formation of recombination centers.[12] Overall, the reported results demonstrate that the total induced alteration of the photocatalytic activity is made up from the sum of changes in intrinsic light-absorption capability of the TiO_2 structure and in charge transfer rate, this latter being governed by the delicate ionic balance of the anatase oxygen sub-lattice. To this extent, one might wonder whether a common spectral denominator, namely a spectroscopic fingerprint, could be found in order to rationalize and to relate to each other the structural characteristics of ionic disorder in TiO_2. Identifying such "fingerprint", which represents the main motivation behind the present study, would allow one categorizing and conceptually binding the successful cases of increased photocatalytic activity against the degradative ones.

One of the main characteristics of CL spectroscopy is the strong excitation induced by the impinged electrons of all the electronic states across the fundamental gap. In other

words, the energy of electrons used in a CL setup is sufficient to excite all luminescence centers in the studied material from the ultraviolet to the infrared region.[13] Furthermore, whereas one incident photon can only generate one electron-hole pair, one incident electron produces a larger number of pairs, which in turn results in up to several orders of magnitude a larger number of photons. Of particular relevance here is that high-energy emissions could be better characterized with using CL as compared to photoluminescence. Note, however, that the large majority of the discussions on the defect structure of TiO_2 films are based on analyses of their photoluminescence spectrum (for a recent review paper see Ref.[14]). Besides oxygen vacancies, which typically emits in the orange/red region,[15,16] an important role is also played by self-trapped excitons (STE) at vacancy sites, which instead should emit much closer (i.e., expected in the violet/blue region) to the fundamental gap. STE were shown to undertake a fundamental function in the overall photocatalytic efficiency of anatase films.[17] Thus, the strong need to efficiently visualize near-band-gap transitions substantiates the importance of CL characterizations in TiO_2 films. Unraveling the specific role and the internal balance of different defect states would mean to remove a major hurdle in designing efficient titania-based photocatalysts, to which purpose the development of a probe for detecting disorder represents a fundamental prerequisite.

II. EXPERIMENTAL TECHNIQUES

Titania thin films were characterized, which were grown by the RF magnetron sputtering technique at room temperature (power density of 15 W/cm^2; pressure of 1.1×10^{-2} mbar; target-substrate distance of 40 mm; angular speed of 140^o/min) either on fused quartz or on soda lime glass substrates (henceforth labeled as Q- and M-samples, respectively). Ti metal (purity better than 99.9 %) was used as a target and the atmos-

phere during growth was kept at 20% partial oxygen pressure, thus leading to oxygen-defective samples after deposition. The final thickness of all the investigated films was 500 nm. Further details about the growth process have been published elsewhere.[18] For comparison with as-grown film samples (labeled T_0), two additional samples for each type of substrate were obtained by annealing the pristine films in air for 1 h at 450^{o}C and 550^{o}C (labeled T_1 and T_2, respectively). Microscopic inspection by atomic force microscopy revealed surfaces with relatively high smoothness for all the investigated samples (surface roughness typically in the range 1~5 nm). The polycrystalline nature of the films with crystal grains, with size typically in the order of the tens of nm, calculated by means of the Scherrer formula, was confirmed by scanning electron micrographs. Figure 1 shows scanning electron micrographs of the deposited films before and after annealing cycles (samples Q and M in (a)/(b) and (c)/(d), respectively). As seen, it is very hard to visualize any microstructural difference among the studied samples by mere microscopic inspection. The annealing cycle in air involved a slight increase in grain size, but such difference could only be detected by X-ray diffraction analyses. Processing conditions and microstructural parameters of the investigated samples are summarized in Table I. X-ray diffractometry and Raman spectroscopy analyses commonly revealed only the presence of anatase phase and concurrently showed a clear increase in crystallinity upon annealing.[18] Estimates of Ti/O ratio could be obtained according to the method given by Parker and Siegel[19] (also listed in Table I). CL spectra were collected in a field-emission gun scanning electron microscope (FEG-SEM, SE-4300, Hitachi Co., Tokyo, Japan) equipped with a CL device. The investigated samples were subjected to preliminary sputtering by platinum (thickness 10 nm) to avoid electron charging effect. Electron irradiation was made with an acceleration voltage of 5 kV and a probe current of 200

pA. Under such conditions, scattering of electrons within the film occurred down to depths at least comparable to the film thickness. Spectral accumulation time was fixed at 20 s. Preliminary calibrations were conducted for optimizing the above CL measurement conditions. According to such calibrations, we found that acceleration voltages <5 kV led to a CL signal of poor and scattered intensity, while voltages >10 kV involved probe-related artifacts, namely damage of the sample upon electron beam impingement. We considered here the occurrence of an instrumental artifacts when by repeating the measurement at the same location , an irreversible difference in the successively recorded spectra could be found (e.g., a change in relative intensity of band components. The CL device consisted of an ellipsoidal mirror and a bundle of optical fibers to collect and to transmit the CL emission into a spectrally resolved monochromator (Triax 320, Jobin-Yvon/Horiba Group, Tokyo, Japan). A grating 150 gr/mm was used throughout the experiments. A liquid-nitrogen-cooled 1024x256 pixels CCD camera was used to analyze the CL emission of the material. Spectral lines were analyzed with the aid of a commercially available software package (Origin v.8.0, OriginLab Co., Northampton, MA, USA). Spectral fitting was conducted by following a deconvolution procedure with Voigtian sub-bands. The CL probe diameter was estimated in the order of 300 nm according to the predicted electron scattering in the material.[20] The CL spectra shown in the remainder of this paper were averaged over about 50 locations randomly selected on each investigated film. In order to evaluate the impact of thermal treatment (and of the ionic disorder) on the functional performance of the films, the degradation rate of an organic phenol substrate was also monitored with subjecting differently annealed samples to an accelerated aging test. Prior to evaluation with respect to their photo-degradation behavior, the film samples were washed, UV irradiated (for 12 h) and dried at 60^{o}C for 15 min. Then, the sam-

ples were embedded in a solution of phenol in nitric acid (at initial concentration, c_0=2x10^{-5} M (pH=3)) that was kept at a constant temperature of 30^{o}C under an UV (wavelength of 360 nm) light source of 33 W/m^2. The details of this procedure are given elsewhere by Minero et al.[21] The chemical composition of the aging solution was then regularly monitored at intervals of 60 s.

III. EXPERIMENTAL RESULTS

CL spectra, which were rigorously collected under exactly the same conditions (and during the same experimental session), are shown in Figs. 2(a) and (b) for M- and Q-type samples, respectively. CL spectra can be thus directly compared with respect to their absolute intensities. As a general trend, the intensity maximum of the overall CL spectrum increased with increasing annealing temperature, as expected according to an increased crystallinity. This assertion is based on studies by Janes et al.,[22] which revealed weak luminescence emission from amorphous TiO_2. In an early paper, Ohtani et al.[23] also reported that the photocatalytic activity of amorphous TiO_2 is negligible, indicating that crystallinity is an important requirement for obtaining efficient samples. The negligible activity of amorphous TiO_2 was attributed to recombination of photoexcited electrons and positive holes at defect sites located on the surface and in the bulk. Our results show that an increase in crystallinity actually involves enhanced luminescence emission, but it does not always relate to an increase in photocatalytic activity (as shown later in this section). Figures 3(a), (b), and (c) show the CL spectra after intensity normalization (and their respective sub-band structures after spectral deconvolution) in the as-deposited and annealed anatase films (M-T_0, M-T_1, and M-T_2, respectively) grown on soda lime glass substrates. CL analyses of anatase films grown on fused quartz substrates are displayed in a similar fashion in

Figs. 3(d), (e), and (f) (for Q-T_0, Q-T_1, and Q-T_2, respectively). More importantly, all spectra could be consistently deconvoluted into three Voigtian sub-bands (labeled *A*, *B*, and *C* in Fig. 3) and clear shape alterations could be observed when comparing the relative intensity of such sub-bands for different samples before and after annealing. Technical details for spectral deconvolution are summarized in Table II and the rationale behind the fitting procedure will be discussed in the next section. In films deposited on soda lime substrates (Figs. 3(a), (b), and (c)), the sub-band located at around 650 nm (labeled sub-band *C*) conspicuously decreased in its relative intensity with respect to the main sub-band *B* (located at around 550 nm) only after annealing at the higher temperature. On the other hand, the sub-band *A* (located at 490 nm) first decreased and then again increased with increasing annealing temperature, while the relative intensity of sub-band *B* remained conspicuously unaltered upon annealing. In films deposited on quartz substrates, a monotonic trend was instead observed for the intensity of sub-band *C*, which gradually decreased with increasing annealing temperature (Figs. 3(d), (e), and (f)). Also in the case of Q-type samples, CL spectra could be deconvoluted with considering the invariance of sub-band *B* upon increasing annealing temperature. Furthermore, unlike films deposited on soda lime substrates, also the relative intensity of sub-band *A* was found to be invariant upon annealing in air.

Figures 4(a) and (b) show the profiles of phenol photo-degradation obtained for the investigated samples of type M and Q, respectively, before and after the annealing cycles. A first-approximation interpolation with straight lines allows one to retrieve a slope, k_0, which is related to the initial phenol degradation rate (i.e., a direct measure of the photocatalytic activity of the film). The retrieved slope values are given in inset to Fig. 4. Pushing the annealing temperatures toward higher values, which was found to increase crystallinity but also to conspicuously alter the relative intensity balance of

CL sub-bands, led either to an increase (Q-type samples) or to a decrease (M-type samples) in the photo-catalytic activity of the film in a way apparently independent of the overall CL emission efficiency. The intrinsic difference in photocatalytic efficiency appears to be related in a complex way to the morphology of the CL spectrum and, in particular, to the reciprocal intensity of the observed sub-bands, as discussed in the next section.

IV. DISCUSSION

CL data of anatase samples are seldom found in the published literature and the interpretation given of the electronic transitions behind their individual sub-bands controversial. In a recent paper, Wu et al.[24] published the CL spectrum of TiO_2 nanowires and found in it three sub-bands: one high-energy band at 418 nm was attributed to STE localized on TiO_6 octahedral (in agreement with Tang et al.[25] and Saraf et al.[26]), while two additional bands at 465 and 536 nm were both attributed to oxygen vacancies (i.e., to F- and F^+-type color centers, respectively). On the other hand, Sekiya et al.[15,16] have given a different interpretation about the physical origin of two luminescence sub-bands emitted by anatase. The emission band located at around 550 nm (corresponding to sub-band *B* in our experiments) was attributed to the relaxation of STE based on the arguments that this sub-band is effectively excited by band-to-band excitation and its intensity is independent of the oxygen annealing procedure. Note that, since representing an intrinsic property of the TiO_2 crystal structure, the STE emission should be independent of oxygen stoichiometry.[27] On the other hand, the emission sub-band located at around 500 nm (i.e., our band *A*) was interpreted as due to excitons bound to reduced titanium ions, interpretation supported by the argument that annealing under oxygen pressure should decrease the concentration of partially

reduced titanium ions (Ti^{3+}) in the crystal lattice. We shall agree here with the assignment given by Sekiya et al.[15] for the observed CL sub-bands. Remarkably, in our deconvolutive procedure for the CL spectra, we were able to fit all the intensity-normalized spectra with no change in relative intensity of the sub-band located at 550 nm, thus confirming its independency of oxygen stoichiometry. The assignment of sub-band *C*, observed in the orange/red region, to optically active oxygen vacancy sites is also supported by absorption studies of anatase films.[1] It follows that, from a phenomenological viewpoint, a decrease in vacancy concentration in the anatase lattice can be revealed by the gradual disappearance of the prominent shoulder located in the low-energy region of the CL spectrum. Following the findings of Sekiya et al.[15], fitting of all CL spectra was performed with considering three sub-bands of Voigtian nature, with maxima located in first approximation at around 490, 550 and 650 nm (cf. Table II) and corresponding to emissions from reduced Ti^{3+} lattice sites, STE, and oxygen vacancy sites, respectively. Since we have observed no emission band in the near-infrared region (>750 nm) in any of the sample examined, we could rule out here the presence of interstitial centers, Ti_i^{3+}, as reported by Plugaru et al.[28]

It is intuitive and has been repeatedly suggested[13,29,30] that luminescence emission and photocatalytic reaction represent different aspects of the same physicochemical behavior of a semiconductor. Hence, the two phenomena should be closely related to each other through the dynamics of photo-stimulated charge-carriers. In general, one would expect that the lower the luminescence emission, the lower the recombination rate of photo-induced electron-hole pairs (i.e., the higher the photocatalytic activity of the material).[13] However, this notion has been disproved for a number of different TiO_2 samples,[13,31] and also the present study shows an inverse trend at least for one of the two investigated sets of samples (cf. Figs. 2 and 3). In particular, in CL experi-

ments we directly inject electrons onto the sample, so we can rather monitor electron-hole recombination processes than photo-induced reactions. Clearly, the details of the electron-hole recombination process are relevant to the photocatalytic efficiency of the film, as they are better represented by the morphology of the CL spectrum than by its mere intensity. The evolution of the spectra in Figs. 3(d), (e), and (f) shows that annealing in air reduces the concentration of oxygen vacancies (as one would conceivably expect) in the anatase films deposited on quartz substrates, while leaving unchanged the concentration of partially reduced Ti^{3+} ions. On the other hand, the trend found upon air annealing for anatase films deposited on soda lime substrates (Figs. 3(a), (b), and (c)) was somewhat unanticipated. A decrease in the concentration of oxygen vacancy was only recorded after annealing at higher temperature, while the concentration of Ti^{3+} ions markedly decreased only upon annealing at 450^{o}C. Hence, the first output of the CL analysis is that the emissions related to Ti^{3+} and to oxygen vacancies do not necessarily experience a correlated behavior, as one would reasonably expect for the equilibrium state, at which the formation of one vacancy generates two Ti^{3+} defects. Obviously, the ionic equilibrium is altered in the M-type set of samples by a strong external factor. Enhanced diffusion profiles of Na^{+} ions, displaced from the soda lime substrate toward the anatase film structure (as detected by secondary ion mass spectrometry in the present films[32]), are the key to interpret the change in ionic disorder in our M-type samples. Na^{+} ions were reported to induce the formation of catalytically inactive titanates,[33] to be responsible for suppressed crystallization,[34] and to induce the formation of recombination centers.[12] Although titanate phases could not be detected in our films, an appreciable effect of Na^{+} ions in delaying crystallization could be found, as shown by the relatively low CL intensity detected after annealing at 450^{o}C in comparison with films deposited on quartz substrates

(cf. relative intensities of CL spectra from samples M-T_1 and Q-T_1 in Figs. 2(a) and (b), respectively). However, CL data newly suggest that diffusion of Na^+ ions from the substrate plays a fundamental role on film stoichiometry with delaying annihilation of oxygen vacancies (while promoting annihilation of Ti^{3+} sites) upon 1 h annealing in air at 450^{o}C. Ionic equilibrium seems to be restored in M-type samples upon treatment for 1 h at 550^{o}C, since annihilation of oxygen vacancies (and the partial re-establishment of the related Ti^{3+} defect sites) is observed, as generally expected in air-annealed samples. CL data could be interpreted in the light of an electron paramagnetic resonance study published by Liu et al.[4] on hydrogen-annealed (undoped) anatase samples. This study reports that the ionic equilibrium at 450^{o}C in anatase requires oxygen vacancies to reach a saturated state before the electrons at vacancy sites could be transferred out to form Ti^{3+} sites. In other words, the optimum H-annealing temperature to produce oxygen vacancies and Ti^{3+} sites is not exactly the same, vacancy formation being thermodynamically preferred at lower temperatures (<520^{o}C) in a reductive atmosphere. On the contrary, in oxidizing atmosphere at temperatures >520^{o}C, formation of new oxygen vacancies is energetically favorable as compared to annihilation of Ti^{3+} sites, which in turn are compensated by intrinsic oxygen-vacancy sites in the material. With the incorporation in the lattice of additional monovalent Na^+ cations, a new negatively charged defect, $\left(Na^{+}_{Ti^{4+}}\right)^{'''}$, is introduced because of the substitution of Na^+ for Ti^{4+} ions, according to the equation:

$$Na^{+} + TiO_2 \rightarrow \left(Na^{+}_{Ti^{4+}}\right)^{'''} + 3h^{\bullet} + O^{x}_{O}, \qquad (1)$$

where the Kröger-Vink notation[35] is used to describe electric charge and lattice position for point defect species and the symbol *h* represents a hole. Accordingly, to preserve electrical neutrality, these defects should be compensated by intrinsic oxygen

vacancies, thus reducing the content of preexisting $\left(\mathrm{Ti}_{\mathrm{Ti}^{4+}}^{3+}\right)^{'}$ defects according to the equation:

$$\left(\mathrm{Ti}_{\mathrm{Ti}^{4+}}^{3+}\right)^{'} + \mathrm{h}^{\bullet} + 2\mathrm{O}_{\mathrm{O}}^{\mathrm{x}} \rightarrow \mathrm{TiO}_2 \,, \qquad (2)$$

or through the formation of new oxygen vacancies, $\mathrm{V}_{\mathrm{O}}^{\bullet\bullet}$, at sufficiently high temperatures:

$$2\mathrm{h}^{\bullet} + 2\mathrm{O}_{\mathrm{O}}^{\mathrm{x}} \rightarrow \mathrm{V}_{\mathrm{O}}^{\bullet\bullet} + \mathrm{O}_2 \,, \qquad (3)$$

while a competing reaction is concurrently ongoing upon annealing in air:

$$\mathrm{V}_{\mathrm{O}}^{\bullet\bullet} + \mathrm{O}_2 \rightarrow 2\mathrm{h}^{\bullet} + 2\mathrm{O}_{\mathrm{O}}^{\mathrm{x}} \,. \qquad (4)$$

A comparison among relative CL intensities of bands A and C in Figs. 3(a) and (b) shows that, upon annealing at 450^{o}C of the Na^{+}-containing samples, the competing effects of oxygen from the annealing atmosphere and Na^{+} diffusing from the substrate (i.e., the former annihilating and the latter forming oxygen vacancies) result in unchanged vacancy concentration, while selectively reducing the presence of Ti^{3+} sites since Eq. (2) prevails. On the other hand, annealing at 550^{o}C satisfies the requirements for the formation of oxygen vacancy, i.e., Eq. (3) is predominant with respect to Eq. (2) and, by the effect of oxygen from the environment, ionic equilibrium is newly restored. As far as the samples belonging to the Q-series are concerned, as expected, a gradual annihilation of oxygen vacancies (i.e., a reduction of the intensity of sub-band C) is observed, according to the incorporation in the lattice of oxygen from the annealing atmosphere. Interestingly, this process apparently leaves the concentration of Ti^{3+} sites (i.e., represented by the intensity of sub-band A) unchanged. The trend for vacancy concentration is thus, conceivably, the opposite of that observed by annealing in hydrogen atmosphere,[4] but the CL spectra also confirm the extremely stable nature of bulk Ti^{3+} sites. Unlike oxygen vacancies, Ti^{3+} centers, when generat-

ed in the bulk of the film by reductive reaction during deposition at high temperature, strongly resist annihilation upon subsequent annealing.[36]

Figure 5 shows a plot of photocatalytic activity (i.e., expressed in terms of phenol degradation rate, $k_0 c_0$) as a function of the relative intensity, I_A/I_C, of sub-band *A* to sub-band *C* in the CL spectrum. The plot, which only includes samples in equilibrium state with their respective substrates, clarifies that the photocatalytic efficiency of anatase tends to increase with increasing the I_A/I_C ratio. Oxygen vacancies and Ti^{3+} sites could be expected to play an equal role in suppressing the recombination of electron hole pairs and hence in extending their individual lifetimes.[8,37] However, Ti^{3+} ions might be incapable of directly transferring surface electrons to adsorbed oxygen molecules.[38,39] Therefore, to interpret the higher catalytic efficiency observed at higher I_A/I_C ratios, as shown in the plot of Fig. 5, one couldn't simply invoke the argument that ionic equilibrium has become imbalanced towards hypostoichiometric compositions. This concept is in line with the results obtained by other researchers[4] suggesting that, when oxygen vacancies were produced alone, the photocatalytic activity of TiO_2 can only improve slightly. CL newly shows that improvement in photocatalytic activity is the result of an appropriate ratio of oxygen vacancies vs. Ti^{3+} sites and gives its quantification for a 500 nm-thick geometry (cf. exponential equation in inset to Fig. 5). Assuming that both vacancies and Ti^{3+} species become mostly oxidized on the TiO_2 surface upon annealing, the increased efficiency found at ratios $I_A/I_C > 2$ implies that surviving Ti^{3+} ions in the bulk of the sample play a fundamental role in the photocatalytic activity of the film. Although photocatalytic oxidation reactions can only occur on the surface of the TiO_2 catalyst, photogenerated charge carriers need to be trapped in the bulk in order to increase photocatalytic efficiency by separating electrons and holes.[40] This is the main function of Ti^{3+} ions and

also the reason why an appropriate balance between Ti^{3+} and oxygen-vacancy sites is needed for gaining an optimized photocatalytic performance.

V. CONCLUSION

In conclusion, we have verified the physical origin of the CL emission from anatase films and demonstrated that the CL spectrum represents a fingerprint of the ionic disorder in TiO_2, which in turn affects photocatalytic activity. Of general validity should be considered the newly proposed fitting algorithm for the CL spectrum of anatase, which is based on the rigorous physical principles underlying the intra-gap behavior of TiO_2 and removes the difficulties found in a previous paper[18] in interpreting CL data.

REFERENCES

[1] N. Serpone, J. Phys. Chem. B **110**, 24287 (2006).

[2] I. N. Martyanov, T. Berger, O. Diwald, S. Rodrigues and K. J. Klabunde, J. Photochem. Photobiol. A: Chem. **212**, 135 (2010).

[3] S.-C. Ke, T.-C. Wang, M.-S. Wong and N. O. Gopal, J. Phys. Chem. B **110**, 11628 (2006).

[4] H. Liu, H. T. Ma, X. Z. Li, W. Z. Li, M. Wu and X. H. Bao, Chemosphere **50**, 39 (2003).

[5] J. C. Yu, J. Lin, D. Lo and S. K. Lam, Langmuir **16**, 7304 (2000).

[6] K. Okamoto, Y. Yamamoto, H. Tanaka, M. Tanaka and A. Itaya, Bull. Chem. Soc. Jpn. **58**, 2015 (1985).

[7] J. E. Rekoske and M. A. Barteau, J. Phys. Chem. B **101**, 1113 (1997).

[8] R. F. Howe and M. Grätzel, J. Phys. Chem. **91**, 3906 (1987).

[9] O. Carp, C. L. Huisman and A. Reller, Progress Solid State Chem. **32**, 33 (2004).

[10] M. Batzill, E. H. Morales and U. Diebold, Phys. Rev. Lett. **96**, 026103 (2006).

[11] M. E. Kurtoglu, T. Longenbach and Y. Gogotsi, Int. J. Appl. Glass Sci. **2**, 108 (2011).

[12] Y. Paz, Z. Luo, L. Rabenberg and A. Heller, J. Mater. Res. **10**, 2842 (1995).

[13] B. G. Yacobi and D. B. Holt, J. Appl. Phys. **59**, R1 (1986).

[14] L. Jing, Y. Qu, B. Wang, S. Li, B. Jiang, L. Yang, W. Fu, H. Fu and J. Sun, Solar En. Mater. Solar Cells **90**, 1773 (2006).

[15] T. Sekiya, S. Kamei and S. Kurita, J. Lumin. **87-89**, 1140 (2000).

[16] T. Sekiya, K. Ichimura, M. Igarashi and S. Kurita, J. Phys. Chem. Solids **61**, 1237 (2000).

[17] T. Berger, M. Sterrer, O. Diwald, E. Knözinger, D. Panayotov, T. L. Thompson and J. T. Yates, Jr., J. Phys. Chem. B **109**, 6061 (2005).

[18] S. Battiston, A. Leto, M. Minella, R. Gerbasi, E. Miorin, M. Fabrizio, S. Daolio, E. Tondello and G. Pezzotti, J. Phys. Chem. A **114**, 5295 (2010).

[19] J. C. Parker and R. W. Siegel, Appl. Phys. Lett. **57**, 943 (1990).

[20] K. Kanaya and S. Okayama, J. Phys. D: Appl. Phys. **5**, 43 (1972).

[21] C. Minero, G. Mariella, V. Maurino and E. Pelizzetti, Langmuir **16**, 2632 (2000).

[22] R. Janes, M. Edge, J. Rigby, D. Mourelatou and N. S. Allen, Dyes and Pigments **48**, 29 (2001).

[23] R. Ohtani, Y. Ogawa and S. I. Nishimoto, J. Phys. Chem. B **101**, 3746 (1997).

[24] J.-M. Wu, H. C. Shih, W.-T. Wu, Y.-K. Tseng and I.-C. Chen, J. Crystal Growth **281**, 384 (2005).

[25] H. Tang, H. Berger, P.E. Schmid and F. Levy, Solid State Commun. **87**, 847 (1993).

[26] L. V. Saraf, S. I. Patil, S. B. Ogale, S. R. Sainkar and S. T. Kshirsager, Int. J. Mod. Phys. B **12**, 2635 (1998).

[27] J. Singh and A. Matsui, Phys. Rev. B **36**, 6094 (1987).

[28] R. Plugaru, A. Cremads and J. Piqueras, J. Phys.: Condens. Matter **16**, S261 (2004).

[29] J. G. Yu, H. G. Yu, B. Chen, X. J. Zhao, J. C. Yu and W. K. Ho, J. Phys. Chem. B **107**, 13871 (2003).

[30] X. Z. Li, F. B. Li, C. L. Yang and W. K. Ge, J. Photochem. Photobiol. A **141**, 209 (2001).

[31] L. Q. Jing, X. J. Sun, B. F. Xin, W. M. Cai and H. G. Fu, J. Solid State Chem. **177**, 3375

(2004).

[32] S. Battiston, Doctoral Thesis, Padua University, Padova, Italy, 2010.

[33] A. Fujishima and T. Rao, J. Chem. Sci. **109**, 471 (1997).

[34] K.-S. Lee and S. H. Lee, Mater. Lett. **61**, 3516 (2007).

[35] F. A. Kröger, H. J. Vink, in *Solid State Physics*, edited by F. Seitz and D. Turnbull, Advances in Research and Applications Volume 3 (Academic Press, New York, 1956) p. 307.

[36] T. Torimoto, R. J. Fox III and M. A. Fox, J. Electrochem. Soc. **143**, 3712 (1996).

[37] S. Ke, T. Wang, M. Wong and N. O. Gopal, J. Phys. Chem. B **110**, 11628 (2006).

[38] Y. Nakaota and Y. Nosaka, J. Photochem. Photobiol. A, Chem. **110**, 299 (1997).

[39] A. M. Czoska, S. Livraghi, M. Chiesa, E. Giamello, S. Agnoli, G. Granozzi, E. Finazzi, C. Di Valentin and G. Pacchioni, J. Phys. Chem. C **112**, 8951 (2008).

[40] A. L. Linsebiger, G. Q. Lu and J. T. Yates Jr., Chem. Rev. **95**, 735 (1995).

FIGURES AND TABLES

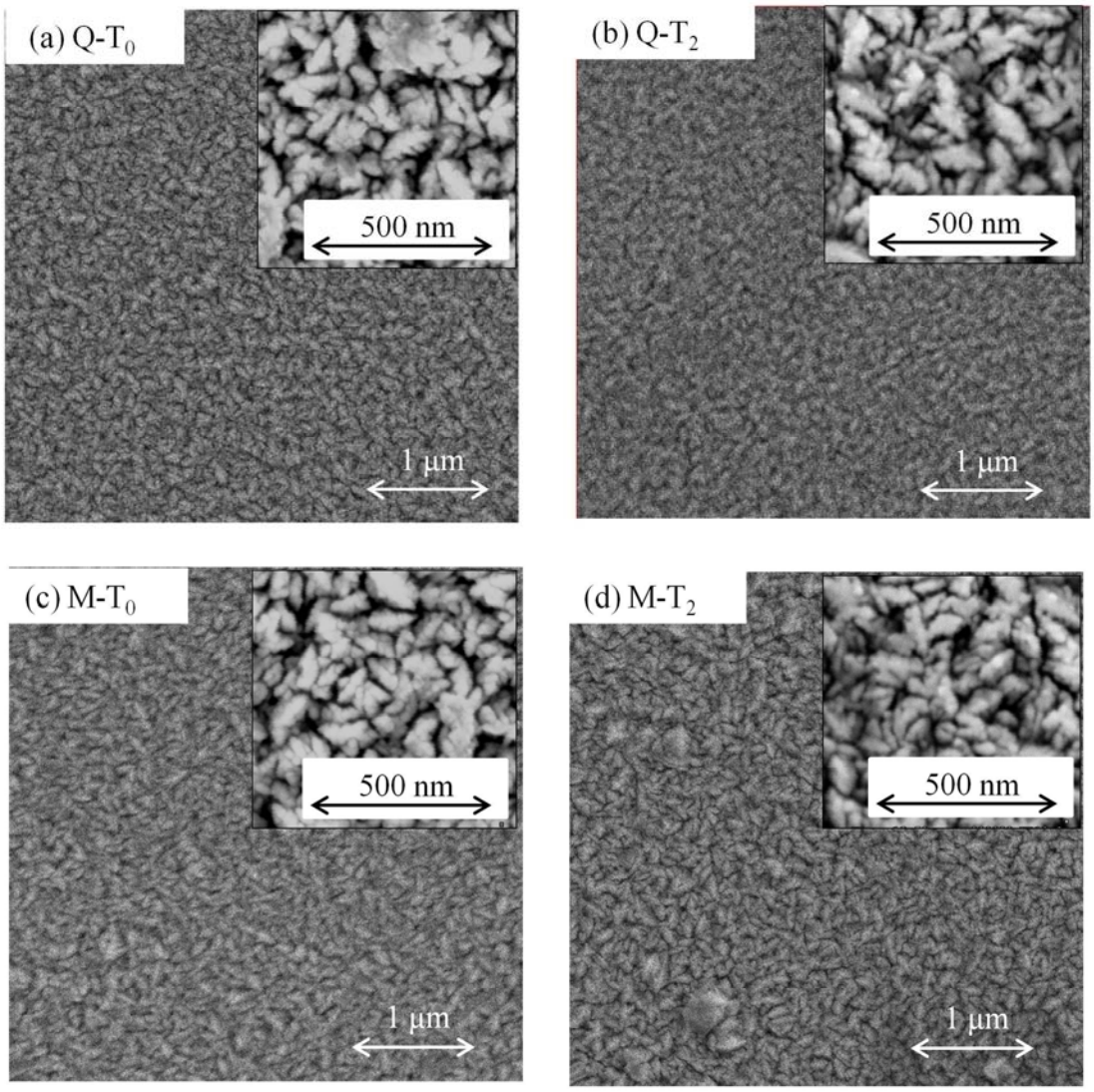

FIG. 1. Scanning electron micrographs of the anatase films before and after annealing in air. Q-type samples are displayed in (a) and (b), while M-type samples in (c) and (d). Each micrograph includes an inset with a higher magnification view of the microstructure.

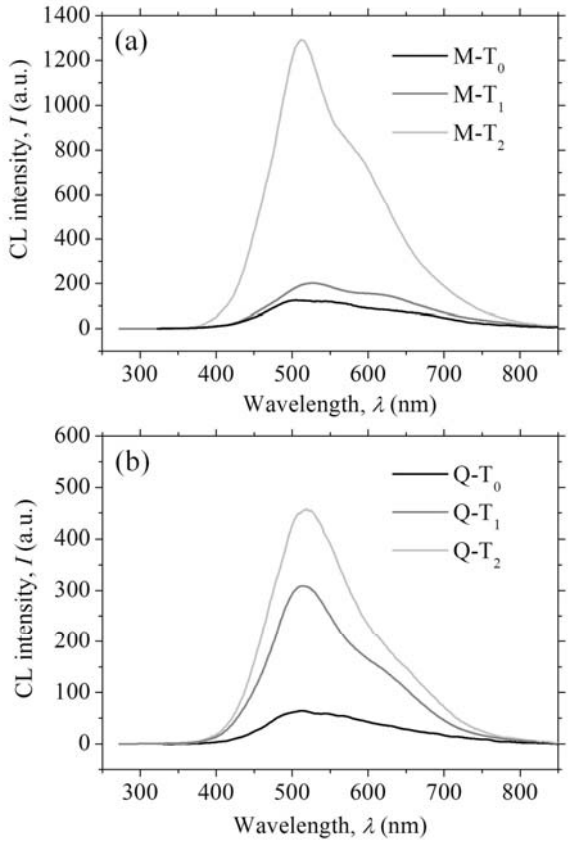

FIG. 2. Average CL spectra representative of M-type and Q-type samples (in (a) and (b), respectively), which were collected under exactly the same experimental conditions before and after annealing cycles at different temperatures.

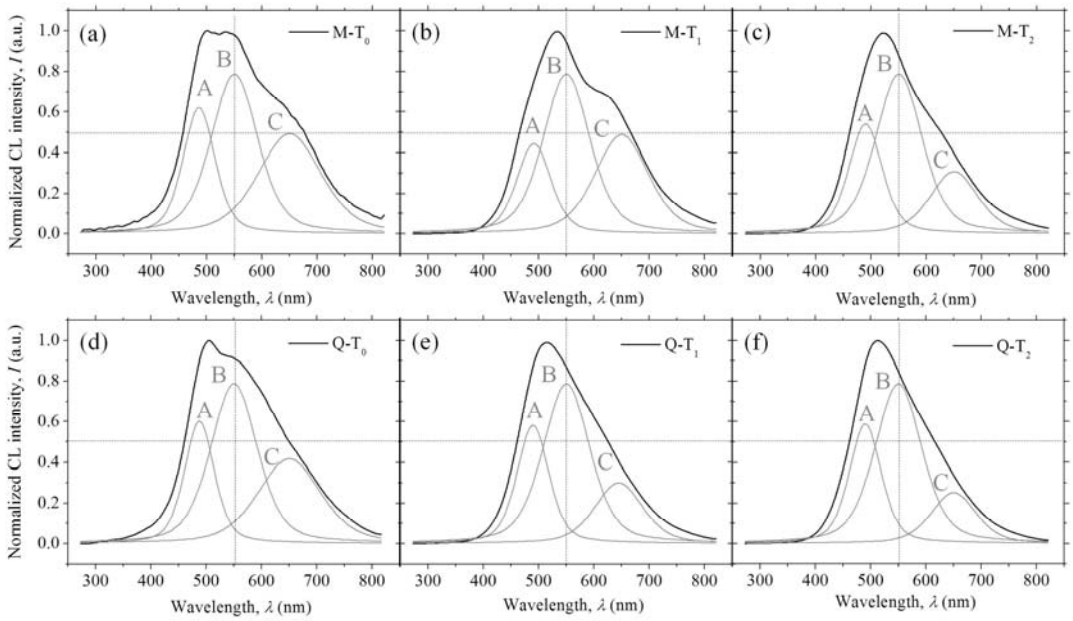

FIG. 3. Average CL spectra as obtained after intensity normalization in the as-deposited and annealed anatase films grown on both soda lime glass ((a), (b), and (c)) and quartz substrates ((d), (e), and (f)). Spectral deconvolution into three Voigtian sub-bands, was applied according to the same criterion (as discussed in Sections III and IV) for all samples.

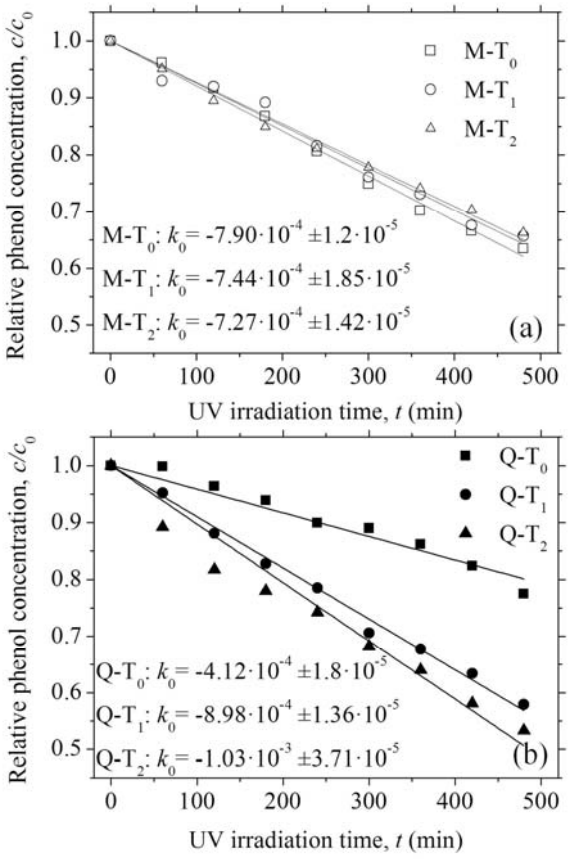

FIG. 4. Profiles of phenol photo-degradation upon UV irradiation as obtained for the investigated samples of M- and Q-type are shown in (a) and (b), respectively. Plots represent the behavior of the samples before and after the annealing cycles. The respective slopes, k_0, of the plots, representing the initial phenol degradation rate, are explicitly listed in inset.

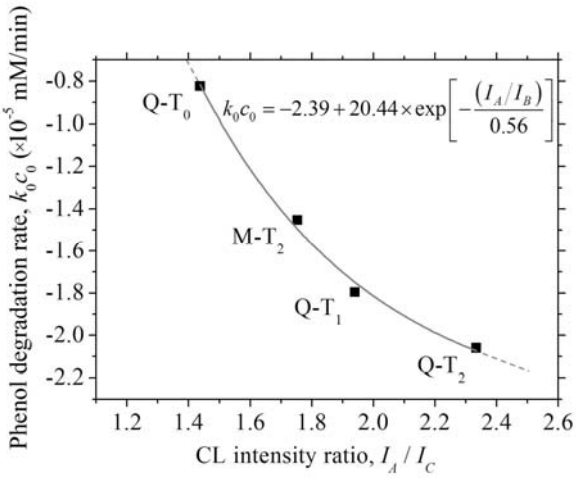

FIG. 5. Phenol degradation rate, k_0c_0, is shown as a function of the relative intensity of sub-band *A* to sub-band *C* (i.e., representing Ti^{3+} and oxygen vacancy defective sites, respectively) in the average CL spectra displayed in Fig. 3. Data can be fitted with high precision to the exponential equation shown in inset.

TABLE I: Processing conditions and microstructural parameters of the investigated film samples.

Sample	Film thickness [µm]	Structure	Substrate	Annealing	Crystallite size [nm]	O/Ti ratio
M-T_0	0.5	Anatase	Soda-lime glass	/	22	1.995
M-T_1	0.5	Anatase	Soda-lime glass	450°C - 1h	35	1.997
M-T_2	0.5	Anatase	Soda-lime glass	550°C - 1h	42	2
Q-T_0	0.5	Anatase	Silica glass	/	33	1.990
Q-T_1	0.5	Anatase	Silica glass	450°C - 1h	40	1.997
Q-T_2	0.5	Anatase	Silica glass	550°C - 1h	43	2

TABLE II: Fitting parameters used for initial input in the nonlinear-curve-fit tool available in the software Origin™ for the three Voigtian sub-bands (program function: PsdVoigt1). The spectral interval, ε, represents a constrained variability interval within the wavelengths in brackets superimposed during fitting for sub-band A. The term "amplitude" refers to a parameter of the program function related to the area subtended by the sub-band. This latter parameter was preliminary optimized to maximize the correlation factor between experimental and fitting spectra (always R>0.998 and Chi-square<$3\cdot10^{-4}$).

Sub-band PsdVoigt1	Peak position, X (nm)		Amplitude, A (a.u.)		Peak width, W (nm)	
	Initial value	Fixed/free	Initial value	Fixed/free	Initial value	Fixed/free
A	490	ϵ [480,500]	50	free	70	free
B	550	fixed	100	fixed	100	fixed
C	650	fixed	50	free	70	free